Genuinely multidimensional evolution Galerkin schemes for the shallow water equations.

Mária Lukáčová-Medviďová and Jitka Saibertová

Institute of mathematics, University of Technology Brno, Technická 2, 616 00 Brno, Czech Republic *lukacova@fme.vutbr.cz, saibertova@mat.fme.vutbr.cz*

1 Introduction

Many types of flows not necessarily involving water, can be characterised as shallow water flows. They describe flows of fluids with a free surface under the influence of gravity, where the vertical dimension is much smaller than any typical horizontal scale. In 1950 von Neumann *et al.* produced first weather forecast by simulating the two-dimensional shallow water equations describing atmospheric flows. Further examples of shallow water are rivers with their flood plains, flows in lakes generated by wind blows, propagation of tsunamis, oceanographic and geophysical flows.

Oceanographic flows were simulated in 1956 by Hansen. Traditionally, tidal flows are computed on the entire globe taking tide-generation forces by sun and moon into account. The prediction of storm surges is also of interest. In particular, flows and water level variations, generated by atmospheric pressure differences and wind stresses on the water surface, are important.

For smooth flows different methods, such as finite difference schemes, finite element methods, or spectral methods perform quite well. Under some assumptions flows with discontinuities can also be computed numerically. For example, tidal bores observed in some rivers or the wave resulting from the bursting of a dam. In this situation, a moving step front develops, which is comparable to a shock wave in aerodynamics. In our work we consider problems involving bores or hydraulic jumps and therefore the aim is to derive such schemes which take the hyperbolic character of the equations into account and allow modelling of discontinuous flows.

Nowadays there are the so-called finite volume methods which are commonly used numerical schemes in order to solve hyperbolic systems of partial differential equations. In the last decade emphasis has been put on the development of genuinely multidimensional finite volume schemes, see, e.g. [1], [2], [5], [6]. In multidimensional flows, there is in general no longer a finite number of propagation of information along the bicharactersitics, but rather infinitely many directions. This has to be taken into account in order to design a reliable multidimensional scheme. Instead of solving one-dimensional Riemann problems in normal directions to cell interfaces the finite volume evolution Galerkin schemes are based on the genuinely multidimensional approach.

In order to evaluate fluxes on cell boundary the approximate solution at cell interfaces is computed by means of an approximate evolution operator using all of the inifinitely many bicharacteristics explicitly into account. This is a novel feature of our method and a genuine generalization of Godunov's ideas. In the second step the finite volume update is done.

2 Shallow water equations and the exact evolution operators

Let us consider a fluid which is incompressible, non-viscous, non-heat conducting and neglect the vertical component of the velocity due to the shallow effects. Then the two-dimensional shallow water equations can be written in the form of a first order hyperbolic system of conservation laws with a source term

$$\frac{\partial \boldsymbol{V}}{\partial t} + \frac{\partial \boldsymbol{F}(\boldsymbol{V})}{\partial x} + \frac{\partial \boldsymbol{G}(\boldsymbol{V})}{\partial y} = \boldsymbol{T}(\boldsymbol{V}), \quad \boldsymbol{x} = (x, y)^T \in I\!R^2, \tag{1}$$

with

$$\boldsymbol{V} = \begin{pmatrix} h \\ hu \\ hv \end{pmatrix}, \quad \boldsymbol{F}(\boldsymbol{V}) = \begin{pmatrix} hu \\ hu^2 + \frac{gh^2}{2} \\ huv \end{pmatrix},$$

$$\boldsymbol{G}(\boldsymbol{V}) = \begin{pmatrix} hv \\ huv \\ hv^2 + \frac{gh^2}{2} \end{pmatrix}, \quad \boldsymbol{T}(\boldsymbol{V}) = \begin{pmatrix} 0 \\ -gh\frac{\partial(H-h)}{\partial x} + fhv \\ -gh\frac{\partial(H-h)}{\partial y} - fhu \end{pmatrix}.$$

Here h denotes the depth of the shallow water, H is the total difference between the bottom solid surface and the free water surface, u, v are components of the depth averaged velocities of the flow, g is the constant of the gravitational acceleration, and f stays for the Coriolis forces. In this contribution we will consider only homogeneous equations, i.e. $\boldsymbol{T} = \boldsymbol{0}$. The study of influence of the source term is our future goal. It can be included into the scheme either by the operator splitting approach or directly in the derivation of the scheme.

In order to derive the exact integral representation of the solution we will rewrite conservative system (1) with $\boldsymbol{T} = \boldsymbol{0}$ in primitive variables. This is the simplest and the most convenient form for studying bicharacteristics of the system away from shocks. By freezing the Jacobian matrices of $\boldsymbol{F}$ and $\boldsymbol{G}$ at a suitable point $\tilde{P} = (\tilde{x}, \tilde{y}, \tilde{t})$ we get the linearized system written in primitive variables

$$\frac{\partial \boldsymbol{U}}{\partial t} + \boldsymbol{A}_1(\tilde{\boldsymbol{U}})\frac{\partial \boldsymbol{U}}{\partial x} + \boldsymbol{A}_2(\tilde{\boldsymbol{U}})\frac{\partial \boldsymbol{U}}{\partial y} = 0, \tag{2}$$

where $\boldsymbol{U}, \boldsymbol{A}_1(\tilde{\boldsymbol{U}})$ and $\boldsymbol{A}_2(\tilde{\boldsymbol{U}})$ are defined by

$$\boldsymbol{U}=\begin{pmatrix}h\\u\\v\end{pmatrix},\ \boldsymbol{A}_1(\tilde{\boldsymbol{U}})=\frac{\mathrm{d}\boldsymbol{F}(\tilde{\boldsymbol{U}})}{\mathrm{d}\tilde{\boldsymbol{U}}}=\begin{pmatrix}\tilde u\ \tilde h\ 0\\ g\ \tilde u\ 0\\ 0\ 0\ \tilde u\end{pmatrix},\ \boldsymbol{A}_2(\tilde{\boldsymbol{U}})=\frac{\mathrm{d}\boldsymbol{G}(\tilde{\boldsymbol{U}})}{\mathrm{d}\tilde{\boldsymbol{U}}}=\begin{pmatrix}\tilde v\ 0\ \tilde h\\ 0\ \tilde v\ 0\\ g\ 0\ \tilde v\end{pmatrix}.$$

In two space dimensions an arbitrary vector $\boldsymbol{n}$ can be written in the form $\boldsymbol{n}=\boldsymbol{n}(\theta)=(n_x,n_y)^T=(\cos\theta,\ \sin\theta)^T\in\mathbb{R}^2$. The eigenvalues of the matrix pencil $\boldsymbol{A}=\boldsymbol{A}_1n_x+\boldsymbol{A}_2n_y$ are

$$\begin{aligned}\lambda_1&=\tilde u\ \cos\ \theta+\tilde v\ \sin\ \theta-\sqrt{g\tilde h},\\ \lambda_2&=\tilde u\ \cos\ \theta+\tilde v\ \sin\ \theta,\\ \lambda_3&=\tilde u\ \cos\ \theta+\tilde v\ \sin\ \theta+\sqrt{g\tilde h},\end{aligned}$$

where $\sqrt{g\tilde h}=\tilde c$ denotes the wave celerity. The corresponding linearly independent right eigenvectors are

$$\boldsymbol{r}_1=\begin{bmatrix}-1\\ \frac{g}{\tilde c}\cos\theta\\ \frac{g}{\tilde c}\sin\theta\end{bmatrix},\ \boldsymbol{r}_2=\begin{bmatrix}0\\ \sin\theta\\ -\cos\theta\end{bmatrix},\ \boldsymbol{r}_3=\begin{bmatrix}1\\ \frac{g}{\tilde c}\cos\theta\\ \frac{g}{\tilde c}\sin\theta\end{bmatrix}.$$

Let $\boldsymbol{R}$ be the matrix of the right eigenvectors. Its inverse reads

$$\boldsymbol{R}^{-1}=\frac{1}{2}\begin{pmatrix}-1&\frac{\tilde c}{g}\cos\theta&\frac{\tilde c}{g}\sin\theta\\ 0&2\sin\theta&-2\cos\theta\\ 1&\frac{\tilde c}{g}\cos\theta&\frac{\tilde c}{g}\sin\theta\end{pmatrix}.$$

Let us define the vector of characteristic variables $\boldsymbol{W}$

$$\boldsymbol{W}=\boldsymbol{R}^{-1}\boldsymbol{U}.$$

Multiplying system (2) by $\boldsymbol{R}^{-1}$ from the left yields the following characteristic system

$$\frac{\partial\boldsymbol{W}}{\partial t}+\boldsymbol{B}_1(\tilde{\boldsymbol{W}})\frac{\partial\boldsymbol{W}}{\partial x}+\boldsymbol{B}_2(\tilde{\boldsymbol{W}})\frac{\partial\boldsymbol{W}}{\partial y}=0,$$

where

$$\boldsymbol{B}_1=\begin{pmatrix}\tilde u-\tilde c\cos\theta&-\frac{1}{2}\tilde h\sin\theta&0\\ -g\sin\theta&\tilde u&g\sin\theta\\ 0&\frac{1}{2}\tilde h\sin\theta&\tilde u+\tilde c\cos\theta\end{pmatrix},$$

$$\boldsymbol{B}_2=\begin{pmatrix}\tilde v-\tilde c\sin\theta&\frac{1}{2}\tilde h\cos\theta&0\\ g\cos\theta&\tilde v&-g\cos\theta\\ 0&-\frac{1}{2}\tilde h\cos\theta&\tilde v+\tilde c\sin\theta\end{pmatrix},$$

and the characteristic variables $\boldsymbol{W}$ are

$$\boldsymbol{W}(\boldsymbol{n})=\begin{bmatrix}w_1\\w_2\\w_3\end{bmatrix}=\boldsymbol{R}^{-1}(\boldsymbol{n})\boldsymbol{U}=\begin{bmatrix}\frac{1}{2}(-h+u\frac{\tilde c}{g}\cos\theta+v\frac{\tilde c}{g}\sin\theta)\\ u\sin\theta-v\cos\theta\\ \frac{1}{2}(h+u\frac{\tilde c}{g}\cos\theta+v\frac{\tilde c}{g}\sin\theta)\end{bmatrix}. \tag{3}$$

The quasi-diagonalised system of the linearised shallow water equations has the following form

$$\frac{\partial \boldsymbol{W}}{\partial t} + \begin{pmatrix} \tilde{u} - \tilde{c}\cos\theta & 0 & 0 \\ 0 & \tilde{u} & 0 \\ 0 & 0 & \tilde{u} + \tilde{c}\cos\theta \end{pmatrix} \frac{\partial \boldsymbol{W}}{\partial x} + \begin{pmatrix} \tilde{v} - \tilde{c}\sin\theta & 0 & 0 \\ 0 & \tilde{v} & 0 \\ 0 & 0 & \tilde{v} + \tilde{c}\sin\theta \end{pmatrix} \frac{\partial \boldsymbol{W}}{\partial y} = \boldsymbol{S} \tag{4}$$

with

$$\boldsymbol{S} = \begin{bmatrix} S_1 \\ S_2 \\ S_3 \end{bmatrix} = \begin{bmatrix} \frac{1}{2}\tilde{h}(\cos\theta \frac{\partial w_2}{\partial y} - \sin\theta \frac{\partial w_2}{\partial x}) \\ g \sin\theta(\frac{\partial w_3}{\partial x} - \frac{\partial w_1}{\partial x}) + g\cos\theta(\frac{\partial w_1}{\partial y} - \frac{\partial w_3}{\partial y}) \\ \frac{1}{2}\tilde{h}(\sin\theta \frac{\partial w_2}{\partial y} - \cos\theta \frac{\partial w_2}{\partial x}) \end{bmatrix}.$$

Let us denote by $\boldsymbol{x}_\ell$ the ℓ-th bicharacteristic corresponding to the ℓ-th equation of system (4). The bicharacteristic $\boldsymbol{x}_\ell$ is defined in the following way

$$\frac{d\boldsymbol{x}_\ell(s)}{ds} = \begin{pmatrix} b^1_{\ell\ell} \\ b^2_{\ell\ell} \end{pmatrix},$$

where $b^1_{\ell\ell}, b^2_{\ell\ell}$ are the diagonal entries of the matrices $\boldsymbol{B}_1, \boldsymbol{B}_2$, respectively. The bicharacteristics $\boldsymbol{x}_\ell$ create the surface of the so-called bicharacteristic cone, see Fig. 1, with the apex $P = (x, y, t + \triangle t)$ and the footpoints

$$\begin{aligned} Q_1(\theta) &= (x - (\tilde{u} - \tilde{c}\cos\theta)\triangle t, y - (\tilde{v} - \tilde{c}\sin\theta)\triangle t, t), \\ Q_2 \equiv P' &= (x - \tilde{u}\triangle t, y - \tilde{v}\triangle t, t), \\ Q_3(\theta) &= (x - (\tilde{u} + \tilde{c}\cos\theta)\triangle t, y - (\tilde{v} + \tilde{c}\sin\theta)\triangle t, t). \end{aligned}$$

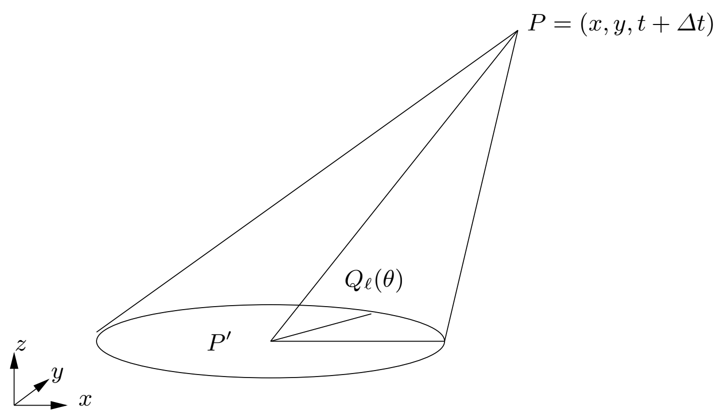

Fig. 1. Bicharacterestics cone.

Integrating each equation of (4) along the corresponding bicharacteristic from the apex P down to the footpoints Q_ℓ we get

$$w_\ell(P) = w_\ell(Q_\ell) + \int_t^{t+\triangle t} S_\ell(Q_\ell(\tilde{t}))\mathrm{d}\tilde{t}, \quad \ell = 1,2,3. \tag{5}$$

Now multiplying (5) with $\boldsymbol{R}$ from the left we go back to the original variables $\boldsymbol{U}$

$$\boldsymbol{U}(P) =$$
$$\frac{1}{2\pi}\int_0^{2\pi} \begin{bmatrix} -w_1(Q_1(\theta),\theta) + w_3(Q_3(\theta),\theta) \\ \frac{g}{\tilde{c}}\cos\theta w_1(Q_1(\theta),\theta) + \sin\theta w_2(Q_2(\theta),\theta) + \frac{g}{\tilde{c}}\cos\theta w_3(Q_3(\theta),\theta)) \\ \frac{g}{\tilde{c}}\sin\theta w_1(Q_1(\theta),\theta) - \cos\theta w_2(Q_2(\theta),\theta) + \frac{g}{\tilde{c}}\sin\theta w_3(Q_3(\theta),\theta)) \end{bmatrix} \mathrm{d}\theta$$

$$+\frac{1}{2\pi}\int_0^{2\pi} \begin{bmatrix} -S_1^{'}(\theta) + S_3^{'}(\theta) \\ \frac{g}{\tilde{c}}\cos\theta S_1^{'}(\theta) + \sin\theta S_2^{'}(\theta) + \frac{g}{\tilde{c}}\cos\theta S_3^{'}(\theta) \\ \frac{g}{\tilde{c}}\sin\theta S_1^{'}(\theta) - \cos\theta S_2^{'}(\theta) + \frac{g}{\tilde{c}}\sin\theta S_3^{'}(\theta) \end{bmatrix} \mathrm{d}\theta, \tag{6}$$

where $S_\ell^{'}(\theta) = \int_t^{t+\triangle t} S_\ell(\boldsymbol{x}_\ell(\tilde{t},\theta),\tilde{t},\theta)\mathrm{d}\tilde{t}$ is an integral along the ℓ-th bicharacteristic.

Since $\lambda_1 = -\lambda_3$, $Q_1(\theta+\pi) = Q_3(\theta)$, and the characteristic variables w_ℓ are 2π-periodic we can, after analogous computations as in [7], reformulate the exact integral equations (6) in the following way

$$h(P) = \frac{1}{2\pi}\int_0^{2\pi} h(Q) - \frac{\tilde{c}}{g}u(Q)\,\cos\theta - \frac{\tilde{c}}{g}v(Q)\,\sin\theta\,\mathrm{d}\theta$$

$$-\frac{1}{2\pi}\int_0^{2\pi}\int_t^{t+\triangle t} \frac{\tilde{c}}{g}S(\boldsymbol{x} - (\tilde{\boldsymbol{u}} - \tilde{c}\boldsymbol{n}(\theta))(t+\triangle t - \tilde{t}),\tilde{t},\theta)\,\mathrm{d}\tilde{t}\,\mathrm{d}\theta, \tag{7}$$

$$u(P) = \frac{1}{2\pi}\int_0^{2\pi} -\frac{g}{\tilde{c}}h(Q)\,\cos\theta + u(Q)\,\cos^2\theta + v(Q)\,\sin\theta\,\cos\theta\,\mathrm{d}\theta$$

$$+\frac{1}{2\pi}\int_0^{2\pi}\int_t^{t+\triangle t} \cos\theta\, S(\boldsymbol{x} - (\tilde{\boldsymbol{u}} - \tilde{c}\boldsymbol{n}(\theta))(t+\triangle t - \tilde{t}),\tilde{t},\theta)\,\mathrm{d}\tilde{t}\,\mathrm{d}\theta$$

$$+\frac{1}{2}u(P') - \frac{g}{2}\int_t^{t+\triangle t} \phi_x(x - \tilde{u}\triangle t, y - \tilde{v}\triangle t, \tilde{t})\,\mathrm{d}\tilde{t}, \tag{8}$$

$$v(P) = \frac{1}{2\pi}\int_0^{2\pi} -\frac{g}{\tilde{c}}h(Q)\ \sin\theta + u(Q)\ \cos\theta\ \sin\theta + v(Q)\ \sin^2\theta\ \mathrm{d}\theta$$

$$+\frac{1}{2\pi}\int_0^{2\pi}\int_t^{t+\triangle t} \sin\theta S(\boldsymbol{x} - (\tilde{\boldsymbol{u}} - \tilde{c}\boldsymbol{n}(\theta))(t+\triangle t - \tilde{t}), \tilde{t}, \theta)\ \mathrm{d}\tilde{t}\ \mathrm{d}\theta$$

$$+\frac{1}{2}v(P') - \frac{g}{2}\int_t^{t+\triangle t} \phi_y(x - \tilde{u}\triangle t, y - \tilde{v}\triangle t, \tilde{t})\ \mathrm{d}\tilde{t}. \tag{9}$$

Here $P = (x, y, t + \triangle t)$, $P' = (x - \tilde{u}\Delta t, y - \tilde{v}\Delta t, t)$, $Q(\theta) = Q_1(\theta) = (x - (\tilde{u} - \tilde{c}\cos\theta)\triangle t, y - (\tilde{v} - \tilde{c}\sin\theta)\triangle t, t)$, and $(\boldsymbol{x} - (\tilde{\boldsymbol{u}} - \tilde{c}\boldsymbol{n}(\theta))(t + \triangle t - \tilde{t})) = (x - (\tilde{u} - \tilde{c}\cos\theta)(t + \triangle t - \tilde{t}), y - (\tilde{v} - \tilde{c}\sin\theta)(t + \triangle t - \tilde{t}))$.
The term S is given by

$$\begin{aligned} S(\boldsymbol{x}, t, \theta) := \tilde{c}[&u_x(\boldsymbol{x}, t, \theta)\sin^2\theta - (u_y(\boldsymbol{x}, t, \theta) + v_x(\boldsymbol{x}, t, \theta))\sin\theta\cos\theta \\ &+ v_y(\boldsymbol{x}, t, \theta)\cos^2\theta]. \end{aligned} \tag{10}$$

3 Approximate evolution operator and the finite volume evolution Galerkin method

Equations (7) - (9) give an implicit exact integral representation of the solution to system (2). In order to derive an explicit numerical scheme we will approximate time-like integrals along bicharacteristics from t up to $t + \Delta t$ by the rectangle rule and evaluate integrands at the old time level t.

Spatial derivatives of velocities u and v appearing in the definition of the term S, cf. (10), can be further eliminating by means of the following lemma, see [2].

Lemma 1. *Suppose $w \in C^1(\mathbb{R}^2)$, and $p \in C^1(\mathbb{R})$ are 2π-periodic. Then integrating round the circle of radius a, with a center having the coordinates (z_1, z_2), $z_1, z_2 \in R$; and denoting a general point by $Q \equiv (z_1 + a\cos\theta, z_2 + a\sin\theta)$, where $z_1, z_2 \in I\!R$, gives*

$$\int_0^{2\pi} p'(\theta)w(Q)\mathrm{d}\theta - a\int_0^{2\pi} p(\theta)[w_x(Q)\sin\theta - w_y(Q)\cos\theta]\mathrm{d}\theta = 0. \tag{11}$$

Proof. Consider the integral of $\frac{\mathrm{d}}{\mathrm{d}\theta}[p(\theta)w(Q)]$, noting $\frac{\mathrm{d}}{\mathrm{d}\theta} = -a(\sin\theta\frac{\partial}{\partial x} - \cos\theta\frac{\partial}{\partial y})$.

■

Taking $p = \sin\theta, w = u$ and $p = -\cos\theta, w = v$ with $a = \tilde{c}\Delta t$, $z_1 = x - \tilde{u}\Delta t$ and $z_2 = y - \tilde{v}\Delta t$ gives from the definition of S in (10)

$$\Delta t \int_0^{2\pi} S(t,\theta)\mathrm{d}\theta = \int_0^{2\pi} [u_Q \cos\theta + v_Q \sin\theta]\mathrm{d}\theta. \tag{12}$$

Analogously we can derive

$$\Delta t \int_0^{2\pi} S(t,\theta)\sin\theta\mathrm{d}\theta = \int_0^{2\pi} [2u_Q \sin\theta\cos\theta + v_Q(2\sin^2\theta - 1)]\mathrm{d}\theta \tag{13}$$

and

$$\Delta t \int_0^{2\pi} S(t,\theta)\cos\theta\mathrm{d}\theta = \int_0^{2\pi} [u_Q(2\cos^2\theta - 1) + 2v_Q \sin\theta\cos\theta]\mathrm{d}\theta. \tag{14}$$

Now using (12) - (14) and the rectangle rule approximation of the time integrals we obtain the following approximations of the exact integral representations (7), (8) and (9)

$$h(P) = \frac{1}{2\pi}\int_0^{2\pi} h(Q) - 2\frac{\tilde{c}}{g}\, u(Q)\,\cos\theta - 2\frac{\tilde{c}}{g} v(Q)\sin\theta\mathrm{d}\theta + O(\Delta t^2), \tag{15}$$

$$\begin{aligned} u(P) = \frac{1}{2}u(P') + \frac{1}{2\pi}\int_0^{2\pi} & - \; 2\frac{g}{\tilde{c}}h(Q)\cos\theta + u(Q)(3\cos^2\theta - 1) \\ & + \; 3v(Q)\sin\theta\cos\theta\mathrm{d}\theta + O(\Delta t^2), \end{aligned} \tag{16}$$

$$\begin{aligned} v(P) = \frac{1}{2}v(P') + \frac{1}{2\pi}\int_0^{2\pi} & - \; 2\frac{g}{\tilde{c}}h(Q)\sin\theta + 3u(Q)\sin\theta\cos\theta \\ & + \; v(Q)(3\sin^2\theta - 1)\mathrm{d}\theta + O(\Delta t^2). \end{aligned} \tag{17}$$

Equations (15) - (17) define an approximate evolution operator $E_{\Delta t}$, which is used in order to compute fluxes at cell interfaces.

Now let us consider for simplicity a uniform discretization of a computational domain consisting of squares of size h. The second order **finite volume evolution Galerkin (FVEG) method** can be defined in the following way

$$\boldsymbol{U}^{n+1} = \boldsymbol{U}^n - \frac{\Delta t}{h}\sum_{k=1}^{2} \delta_{x_k}\boldsymbol{F}_k(\boldsymbol{U}^{n+1/2}), \tag{18}$$

where $\boldsymbol{U}^n$ is a piecewise constant approximation of the exact solution at time step t_n, $\delta_{x_k}\boldsymbol{F}_k(\boldsymbol{U}^{n+1/2})$ represents an approximation to the edge flux difference at the intermediate time level $t_n + \Delta t/2$. The cell boundary flux $\boldsymbol{F}_k\left(\boldsymbol{U}^{n+1/2}\right)$ is evolved using the approximate evolution operator $E_{\Delta t/2}$ to $t_n + \Delta t/2$ and averaged along the cell boundary. Thus, e. g., on vertical edges for $\boldsymbol{U}$ itself we have

$$\boldsymbol{U}^{n+1/2} = \frac{1}{h}\int_0^h E_{\Delta t/2} R_h \boldsymbol{U}^n \mathrm{d}S_y. \tag{19}$$

We have denoted by R_h a conservative discontinuous piecewise bilinear recovery, which is constructed using the vertex values, see, e.g. [3], [5] for a detailed description.

In order simplify the evaluation of fluxes along the cell interfaces it is suitable to approximate cell interface integrals from 0 to h appearing in (19) by some suitable numerical quadrature. Let us consider a natural CFL number $\nu = \max(|\tilde{u}| + \tilde{c}, |\tilde{v}| + \tilde{c})\Delta t/h <= 1$. Then the midpoint rule approximation of cell interface integrals naturally does not take into account corner effects since the fluxes are evaluated at $t^n + \Delta t/2$ and thus the cone radius is $\tilde{c}\Delta t/2$. Therefore this quadrature rule is inappropriate for a multidimensional scheme. It is proven in [4] that also the trapzeoidal rule is not appropriate for problems with arbitrary advection velocities $\tilde{u},\ \tilde{v}$, since it leads to a non-monotone scheme. This fact is also demonstrated by numerical experiment in the next section. On the other hand, the Simpson rule approximation of the cell interface integrals leads to a monotone finite volume scheme, see [4] for more details.

In order to construct local bicharacteristic cones we need to determine linearized local flow information $\tilde{u}, \tilde{v}, \tilde{c}$. Put the linearization point $\tilde{P}$ at the cone appex P, i.e. $\tilde{t} = t^n + \Delta t/2$. For the scheme with the Simpson rule approximation of cell interface integrals the points $\tilde{P} \equiv P$ are put in the cell vertices as well as the midpoints of the cell interfaces. Local flow velocities $\tilde{u}, \tilde{v}, \tilde{c}$ can be computed, e.g. by averaging over four cells adjacent to the vertex or over two cells adjacent to the midpoint, respectively.

Further integrals with respect to θ, i.e. along the bicharacteristic cone, will be computed exactly, such that all of the infinitely many directions of bicharactetristics are taken into account explicitly.

4 Numerical experiment: Dam break problem

Solving a rotationally-symmetric problem on a Cartesian grid causes problems for many numerical schemes. Typically a grid aligned effects appear. In this section we present behaviour of the FVEG scheme by solving the so-called dam break problem. A circular dam separating two stationary water levels is suddenly removed and rotationally-symetric waves propagate into these two domains.

We consider a square computational domain $[-1, 1] \times [-1, 1]$ with initial data

$$\begin{aligned} h = 1, \quad u = 0, \quad v = 0, \quad \|\boldsymbol{x}\| < 0.3 \\ h = 0.1, \quad u = 0, \quad v = 0, \quad \text{else.} \end{aligned}$$

Computational domain is divided into 200×200 square cells and numerical solution is computed at time $T = 0.19$. CFL number is set to 0.55. Fig. 2 illustrates contour plots of water depth h and $x-$, $y-$ velocities u and v, respectively. We can notice a circular shock wave, the so-called hydraulic jump, which expands outward of the centre. A circular rarefaction wave is developed within this circular shock. This drains fluid from the original deep region to feed the shock. We have compared two versions of the second order FVEG scheme. The cell interface integrals of fluxes in (19) are approximated either by the Simpson rule (left part) or by the trapezoidal rule (right part). As already mentioned above the trapezoidal rule is inappropriate and leads to oscillations in solution. This is not the case of the FVEG scheme, which uses the Simpson rule. Here the numerical solution preserves rotational symmetry in a perfect way and the problem is solved correctly. Note that in this example the Froude number $\mathrm{Fr} = |\boldsymbol{u}|/c$ is sometimes less and sometimes greater than 1. Thus the subcritical and supercritical flows develop. The FVEG scheme does not need any artifical entropy fix correction in order to resolve the so-called transcritical rarefaction wave correctly.

Acknowledgement

The present research has been supported by the VolkswagenStiftung agency, DFG-grant No. Wa 633/6-2, as well as by the Grants GAČR 201/00/0557, and CZ 39001/2201 of the University of Technology, Brno.

References

1. Fey, M. (1998): Multidimensional upwinding, Part II. Decomposition of the Euler equations into advection equations. J. Comp. Phys., **143**, 181–199
2. Lukáčová - Medviďová, M., Morton, K.W., Warnecke, G. (2000): Evolution Galerkin methods for hyperbolic systems in two space dimensions. Math-Comp., **69**, 1355–1384
3. Lukáčová - Medviďová, M., Morton, K.W., Warnecke, G. (1999): Finite volume evolution Galerkin methods for multidimensional hyperbolic problems. In Vilsmeier, R. et al. (eds.) Finite Volumes for Complex Applications, Hermès
4. Lukáčová - Medviďová, M., Morton, K.W., Warnecke,G.: High-order evolution Galerkin schemes for multidimensional hyperbolic systems. in preparation
5. Lukáčová - Medviďová, M., Saibertová, J., Warnecke,G.: Finite volume evolution Galerkin methods for nonlinear hyperbolic systems. submitted to J. Comp. Phys.
6. Noelle, S. (2000): The MOT-ICE: a new high-resolution wave-propagation algorithm for multi-dimensional systems of conservative laws based on Fey's method of transport. J. Comput. Phys., **164**
7. Ostkamp, S. (1995): Multidimensional characterisitic Galerkin schemes and evolution operators for hyperbolic systems. PhD thesis, Universität Hannover

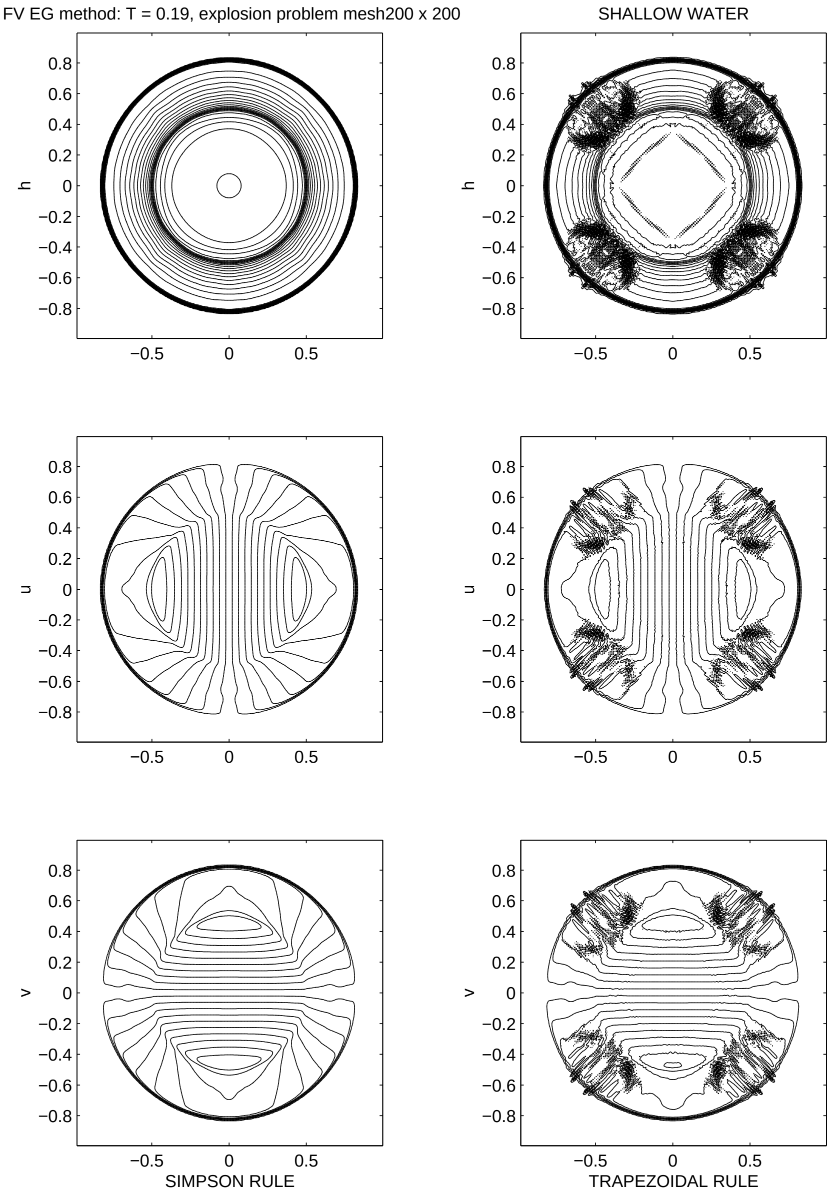

Fig. 2. Isolines of the solution obtained by the second order FVEG scheme with the Simpson rule (left) and the trapezoidal rule (right) at $T = 0.19$ on a 200×200 mesh.